Periodic bedrock ridges on Mars

David R. Montgomery,[1] Joshua L. Bandfield,[1] and Scott K. Becker[1]

Received 22 September 2011; revised 13 January 2012; accepted 14 January 2012; published 9 March 2012.

[1] Evidence for sediment transport and erosion by wind is widespread over the surface of Mars today and was likely a major geomorphic process for much of its geological past. Although Martian surface features resembling aeolian dunes and ripples have been recognized since the Mariner and Viking missions, such features have been interpreted previously as active, indurated, or exhumed sedimentary forms. Here we report evidence based on High Resolution Imaging Science Experiment images that show some megaripple forms are eroded into cohesive substrate rather than being composed of loose granular material or fossilized dunes. Exposure of stratigraphic continuity within layered, cohesive material extending crest to trough through features with mean wavelengths of 18 to 51 m demonstrates the primarily erosional formation of what we term periodic bedrock ridges (PBRs). Hence some surfaces on Mars previously considered to be covered by wind-deposited material are actually wind-carved exposures that offer windows into Martian history. PBRs lack the distinctive streamlining associated with wind-parallel yardangs and comparison of PBR orientation to yardangs, megayardangs, and active sedimentary dunes in the same vicinity confirm that these PBRs formed transverse to prevailing winds. Observed wavelengths of PBRs are comparable to those predicted by a simple model for erosional wavelengths of periodic transverse bed forms owing to the spacing of flow separations within the flow. Recognition of these transverse aeolian erosional forms brings up the question of how widespread Martian PBRs are and how many have been misinterpreted as active or indurated (fossilized) sedimentary dunes.

Citation: Montgomery, D. R., J. L. Bandfield, and S. K. Becker (2012), Periodic bedrock ridges on Mars, *J. Geophys. Res.*, *117*, E03005, doi:10.1029/2011JE003970.

1. Introduction

[2] At a fundamental level, planetary surfaces may be divided into areas of eroding cohesive materials (bedrock) and those that are active sedimentary surfaces shaped by the interplay of erosion, transport, and deposition of loose, particulate materials. Aeolian dunes were first recognized on Mars in Mariner 9 images [*McCauley et al.*, 1972; *Cutts and Smith*, 1973], and have subsequently been documented to be widespread [*Carr*, 1981; *Greeley et al.*, 1992; *Malin and Edgett*, 2001]. Although wind-streamlined yardangs and faceted ventifacts have been observed to be common erosional features on Mars [e.g., *Greeley et al.*, 1992; *Bridges et al.*, 1999; *Thomson et al.*, 2008], dune and ripple forms on Mars generally have been interpreted as sedimentary forms [*McCauley et al.*, 1972; *Cutts and Smith*, 1973; *Carr*, 1981; *Greeley et al.*, 1992; *Malin and Edgett*, 2001] (for a discussion of possible misinterpretation of ripple-like landforms, see *Balme et al.* [2008]). While the presence of active aeolian dunes has been clearly established on Mars [*Bridges et al.*, 2007], and analyses based on HiRISE images document migration of dark sand organized into dunes and ripples [*Silvestro et al.*, 2010; *Chojnacki et al.*, 2011; *Hansen et al.*, 2011], some morphologically similar features have exhibited no detectable motion over time spans exceeding several decades [*Zimbelman*, 2000]. Features with megaripple morphology have also been interpreted to be exhumed fossil dunes owing to their cratered and degraded surfaces [*Edgett and Malin*, 2000]. High-resolution images from the Mars Orbiter Camera (MOC) [*Malin and Edgett*, 2001] revealed distinctive light-toned transverse aeolian ridges (TARs) with typical wavelengths of 10–60 m and amplitudes estimated at 2–8 m, the origin of which has been assumed to be aeolian transport and deposition of granular material [*Malin and Edgett*, 2001; *Bourke et al.*, 2006, 2010; *Wilson and Zimbelman*, 2004; *Balme et al.*, 2008; *Zimbelman*, 2010; *Berman et al.*, 2011]. However, there are three possible origins for such features: (1) the conventional interpretation of active interplay among aeolian transport, deposition, and erosion of granular materials; (2) indurated, inactive or exhumed fossil dunes; and (3) primary erosional features carved into cohesive material (bedrock). Of these three possible origins, the first two have been clearly established for some such features on Mars. The third formation mechanism, erosion into cohesive substrate, to our knowledge has not been considered previously. Although a wide array of erosional bed forms carved into cohesive substrates

[1]Department of Earth and Space Sciences, University of Washington, Seattle, Washington, USA.

0148-0227/12/2011JE003970

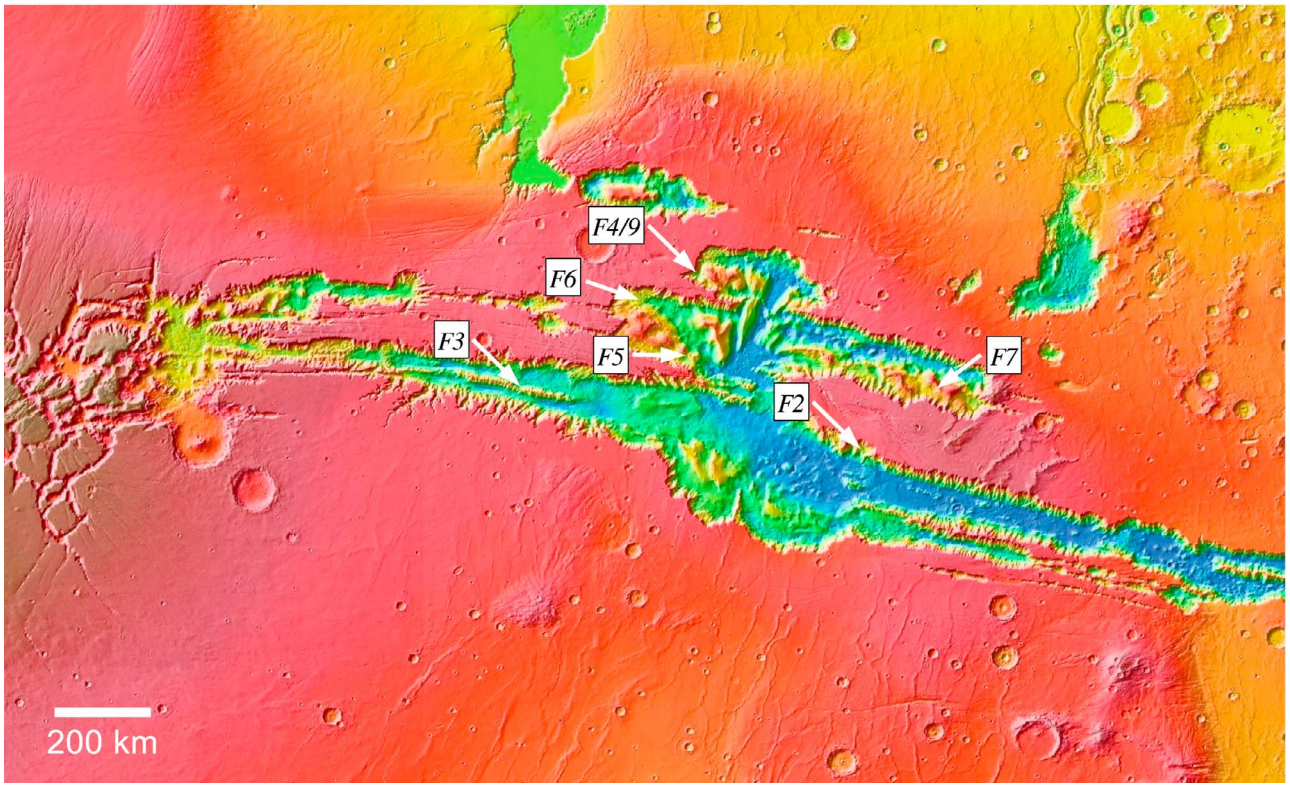

Figure 1. Location map (Mars Orbiter Laser Altimeter shaded relief) showing the study area and locations of images within Valles Marineris in Figure 2 (F2), Figure 3 (F3), Figure 4 (F4), Figure 5 (F5), Figure 6 (F6), Figure 7 (F7), and Figure 9 (F9).

is recognized for terrestrial fluvial systems [*Allen*, 1969, 1971; *Richardson and Carling*, 2005], aeolian landforms resembling dunes and ripples carved into bedrock have only recently been recognized on Earth [*Milana*, 2009].

2. Observations of Periodic Bedrock Ridges

[3] Evidence from High Resolution Imaging Science Experiment (HiRISE) [*McEwen et al.*, 2007] images of Coprates, Ius, Candor, and Ophir chasmas in the region of Valles Marineris (Figure 1) and outcrops of the Medusae Fossae formation northeast of Apollinaris Mons show that some Martian megaripples are eroded into cohesive materials and thus are not sedimentary features but are periodic bedrock ridges (PBRs). HiRISE provides images with a spatial sampling of ~25–50 cm, a level of detail unavailable before the arrival of the Mars Reconnaissance Orbiter (MRO) at Mars. Observations of cratered surfaces on megaripple forms, structural/bedding lineations cutting across ridges from crest to trough, apparent material continuity across transitions to undissected terrain and yardangs, the specific shape of ripple forms in relation to yardangs, and the relationship of ridge orientation to yardangs, megayardangs, and active sedimentary dunes all point toward interpreting PBRs as transverse aeolian erosional features (Table 1). The images discussed below are drawn from a nonsystematic search of HiRISE images in the vicinity of Valles Marineris and the Medusae Fossae Formation, and close inspection of selected areas within those images. Consequently, our analysis does not address whether PBRs are isolated geographically or how extensively they may occur in other areas of Mars.

[4] Previously, craters preserved on ripple forms have been interpreted as fossil dunes [*Edgett and Malin*, 2000]. An example of one such place is the floor of Coprates Chasma where a rhythmic sequence of megaripple-like forms made of cohesive material is disrupted by well-preserved craters

Table 1. Figures That Contain Surface Features/Characteristics Pertinent to Interpretation of PBRs as Transverse Aeolian Erosional Features[a]

Surface Characteristics	Figure 2	Figure 3	Figure 4	Figure 5	Figure 6	Figure 7	Figure 8	Figure 9
Created surfaces	yes	yes					yes	
Through-cutting layers		yes	yes	yes	yes			yes
Orientation relative to sedimentary dunes		yes		yes	yes			
Orientation relative to yardangs						yes	yes	yes
Orientation relative to dominant wind	yes	yes		yes	yes	yes	yes	yes
Continuity with neighboring terrain		yes	yes	yes	yes	yes	yes	yes

[a]"Yes" indicates the figure shows surface characteristics consistent with interpretation as PBRs.

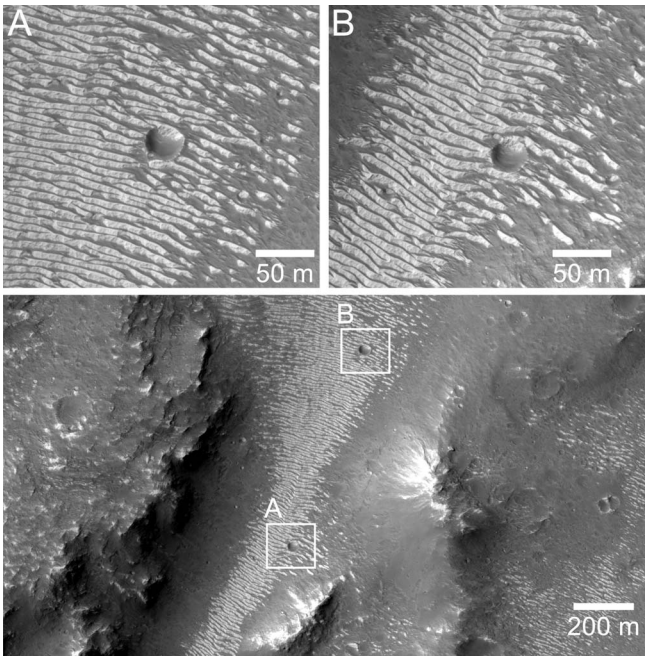

Figure 2. HiRISE image of cohesive, cratered dune-like features on the north wall of Coprates Chasma (PSP_007825_1700_RED, centered near 10.0°S, 291.3°E).

(Figure 2). Relatively low-albedo (dark) wind-blown sand mantles some of the relatively high-albedo (light) ripple forms and fills in portions of the troughs and craters, demonstrating the ability of modern winds to transport the darker material without disrupting the lighter-toned material composing megaripple forms. Hence, these light-toned megaripple-like features scarred and disrupted by craters are a cohesive surface that, if originally formed by sedimentary processes, has been cemented and inactive for some time. Examination of the overview image shows these features to be present on the floor of an incised canyon down which winds would be channeled; they lie transverse to the local prevailing winds. Although the interpretation of the formation mechanism of these features is ambiguous, the possibility of an erosional origin provides an alternative hypothesis to the interpretation of fossil dunes offered to explain similar features identified elsewhere on Mars [*Edgett and Malin*, 2000].

[5] In the cases discussed below, the nature of the material that megaripple-like features are composed of, together with their orientation relative to other, independent indicators of prevailing wind directions supports their interpretation as PBRs.

[6] The presence of discordant layering within the material forming periodic ridges precludes a sedimentary origin for these landforms (though not for the origin of the now-indurated material into which they are carved). One such location on the floor of Ius Chasma reveals more direct evidence for periodic ridges that are carved into two separate topographic faces on a cohesive substrate (close-up image in Figure 3, top). In this location, several craters that disrupt megaripple-like forms and the abundant fractures apparent in the substrate demonstrate the cohesive nature of the material composing the ripple forms. Material discontinuities within the substrate run across and through the full trough-to-crest relief, supporting the interpretation that these megaripple-like forms are incised into cohesive substrate. The development of PBRs on two distinct topographic facets, one eroded into the other (Figure 3, top) show that these PBRs are not exhumed sedimentary forms. These linear ridges lack the distinctive streamlining associated with yardangs, features present elsewhere in this image that provide independent indicators of wind direction. Examination of the overview image reveals that PBRs occur in topographic lows that correspond to areas where an undissected capping layer strong enough to hold near-vertical cliffs has been breached. The PBRs shown in the inset in Figure 3 (top) are generally aligned with the darker dune forms apparent in other portions of the overview image (bottom). We interpret many of these darker forms as active sedimentary dunes of typical transverse dune fields. Hence, the PBRs we identified above appear to be oriented transverse to the prevailing winds.

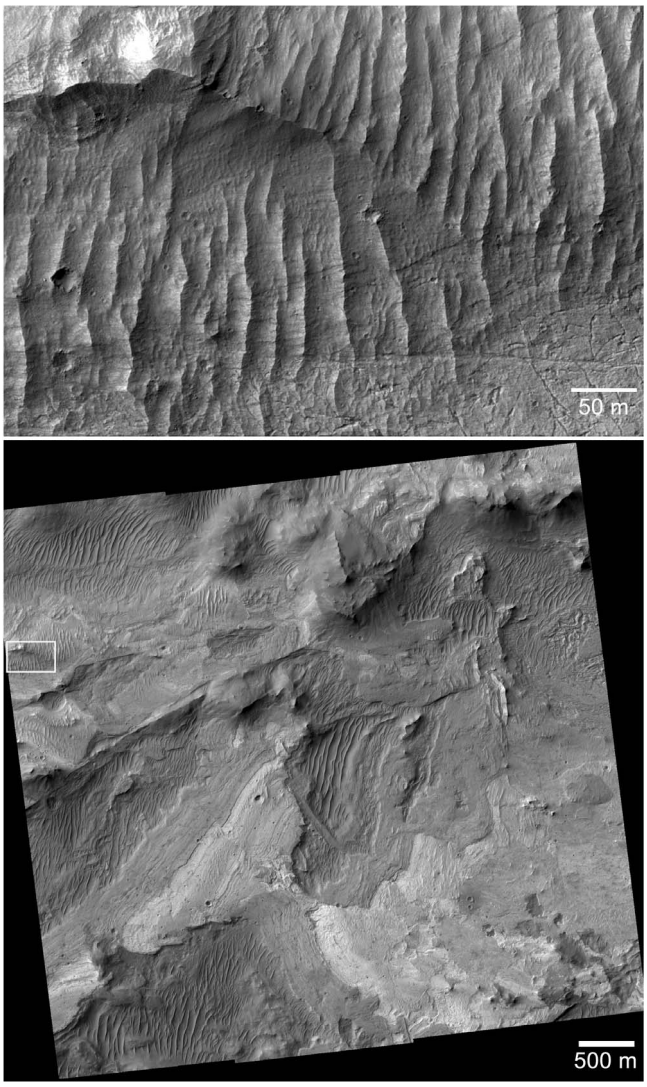

Figure 3. HiRISE image of the floor of Ius Chasma showing cohesive substrate shaped into periodic bedrock ridges as demonstrated by the cratered surface and the material discontinuities running through and across megaripple forms (TRA_000823_1720_RED, centered near 7.7°S, 279.5°E).

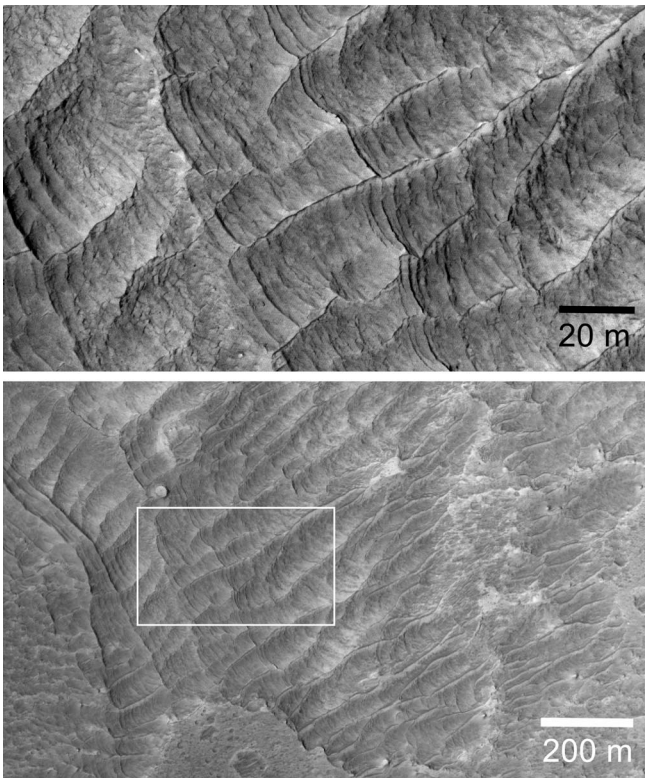

Figure 4. HiRISE image of the interior of West Ophir Chasma showing transverse ridges carved into layered cohesive substrate striking orthogonal to the erosional surface forms (ESP_015974_1760_RED, centered near 3.9°S, 285.7°E).

[7] The floor of West Ophir Chasma similarly exhibits transverse ridges carved into layered cohesive substrate to form PBRs (Figure 4). In Figure 4 (top) the layered substrate strikes orthogonal to periodic ridges running from lower left to upper right. Variable erosion resistance to the layered substrate results in a series of highstanding, erosion-resistant ribs that extend uninterrupted through multiple topographic troughs and ridgecrests. As these PBRs are developed where the hard, cratered capping layer of a plateau remnant has been eroded (lower center of overview image), we consider it likely that here too breaching of a resistant layer exposed weaker underlying material to wind erosion. The crests of individual PBRs bifurcate or coalesce downslope in a manner typical of transverse ripples but unusual for either yardangs or linear, flow-parallel dunes. Several prominent streamlined forms are present in the southeastern portion of the image that appear to have been formed via wind erosion. PBRs immediately adjacent to these forms strike perpendicular to the long axis of the streamlined forms, again indicating the transverse nature of the megaripple forms. The numerous PBRs throughout this image show that such features are common at least in certain areas of Mars.

[8] Another example of megaripple-like forms incised into cohesive material comes from the floor of West Candor Chasma (Figure 5) where both aeolian sedimentary megaripples (dark forms in upper left and right of the overview image) and periodic bedrock ridges (top) are present. The latter are carved into layered stratigraphy that strikes across and extends trough to crest through the PBRs. The interaction of the layers and PBRs shows the presence of an apparent folded structure (or local topographic low) in the bedrock stratigraphy (Figure 5, top). Some ridgecrests appear to be locally enhanced by dark material like that forming active aeolian dunes, suggesting that some PBRs form by a mixed mechanism of active aeolian transport, deposition, and erosion of underlying cohesive substrate (bedrock). These megaripple forms also lack the streamlined form characteristic of yardangs. Examination of the overview image shows that PBRs are aligned parallel to, and track spatial variations in the orientation of proximal megaripples in both the upper left and upper right of the overview image. That the alignment of the erosional features parallels those of active sedimentary dunes supports the interpretation that these PBRs were carved by contemporary prevailing winds. The low-albedo material drapes local topographic features and is smooth and featureless at the scale of the HiRISE images, characteristics typical of active sand deposits that maintain smooth, relatively dust-free cohesionless surfaces via saltation.

[9] The orientation of PBRs parallel to active transverse aeolian dunes is particularly well illustrated in an image of the floor of West Candor Chasma (Figure 6). Here NE-SW oriented dunes of dark material form an active sedimentary dune field across the lower half of the overview image, with

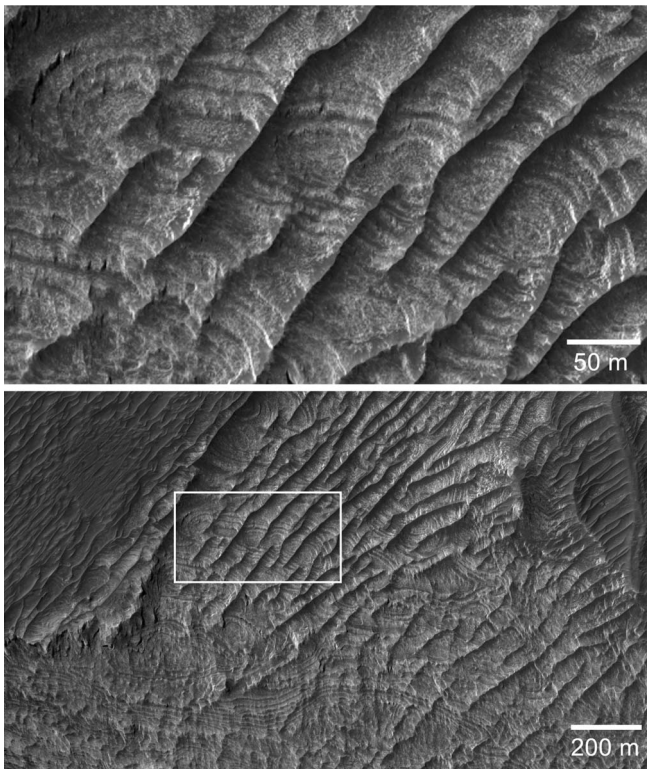

Figure 5. HiRISE image of the floor of West Candor Chasma showing layered stratigraphy exposed from troughs to crests of periodic bedrock ridges, with aeolian sand locally enhancing crests (PSP_008313_1730_RED, centered near 7.0°S, 285.9°E).

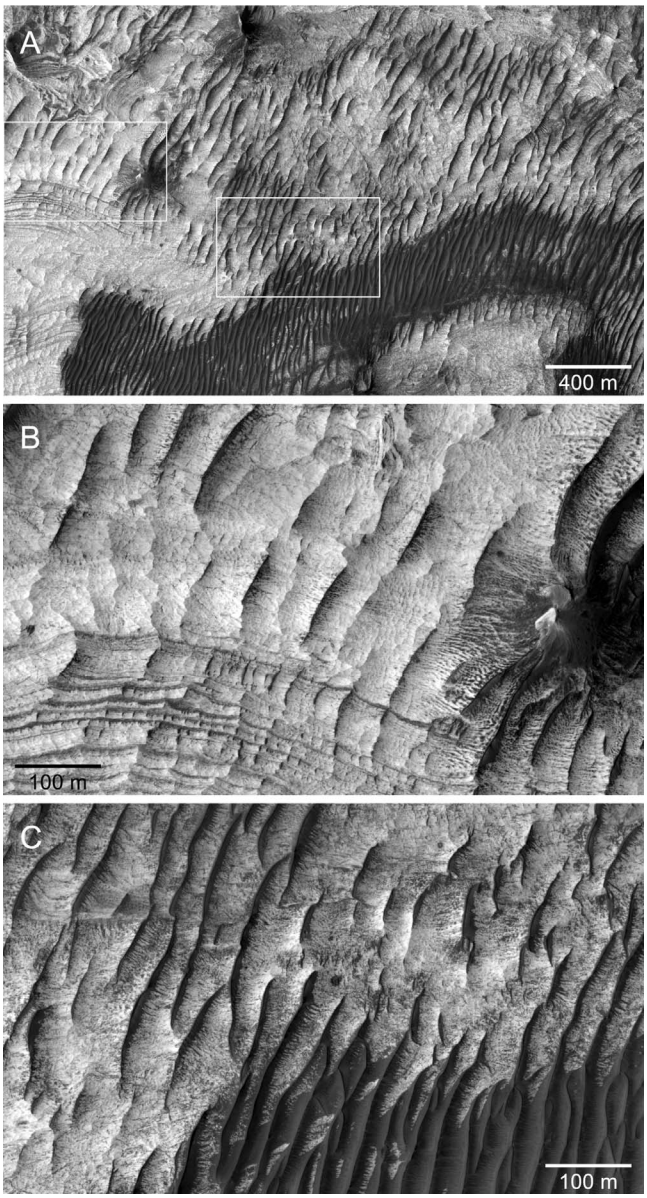

Figure 6. HiRISE image of West Candor Chasma showing layered stratigraphy exposed from troughs to crests of periodic bedrock ridges oriented parallel to active sedimentary dunes (PSP_006164_1750_RED, centered near 4.8°S, 283.5°E). Note deflection of PBRs around topographic knob on the right side of Figure 6b.

a prevailing wind direction of left to right inferred from accumulation of wind-blown dark material on the lee side of PBR crests and the topographic knob (right-hand side of Figure 6b). Clear layering in the cohesive light-toned material extends from crest to trough through numerous PBRs (Figure 6b). In addition, the deflection of PBR crests around topographic knobs formed of apparently the same (bedrock) material favors the interpretation that these PBRs do not represent exhumed depositional features. Active aeolian transport over PBRs is demonstrated by accumulations of dark wind-blown material in the lee of PBR crests (Figure 6c), where PBR orientations parallel those of adjacent active aeolian dunes.

[10] The orientation of PBRs transverse to megayardangs is apparent in features carved into the floor of valleys incised into the flanks of East Candor Chasma (Figure 7). There, streamlined spines of rock with blunt upslope faces and

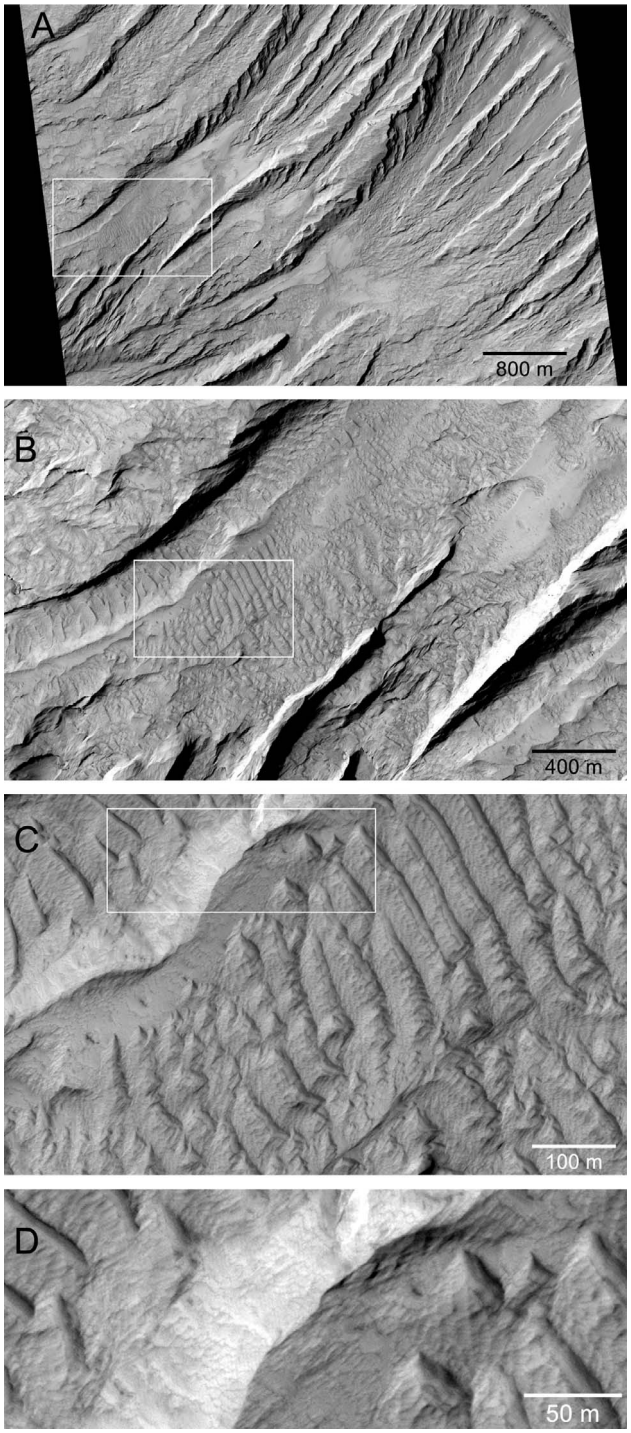

Figure 7. HiRISE image of East Candor Chasma showing asymmetric periodic bedrock ridges oriented transverse to yardangs and megayardangs (PSP_006546_1720_RED, centered near 8.0°S, 293.9°E). Note apparent material continuity from periodic bedrock ridges to adjacent yardang margins in Figure 7d (greatest enlargement image).

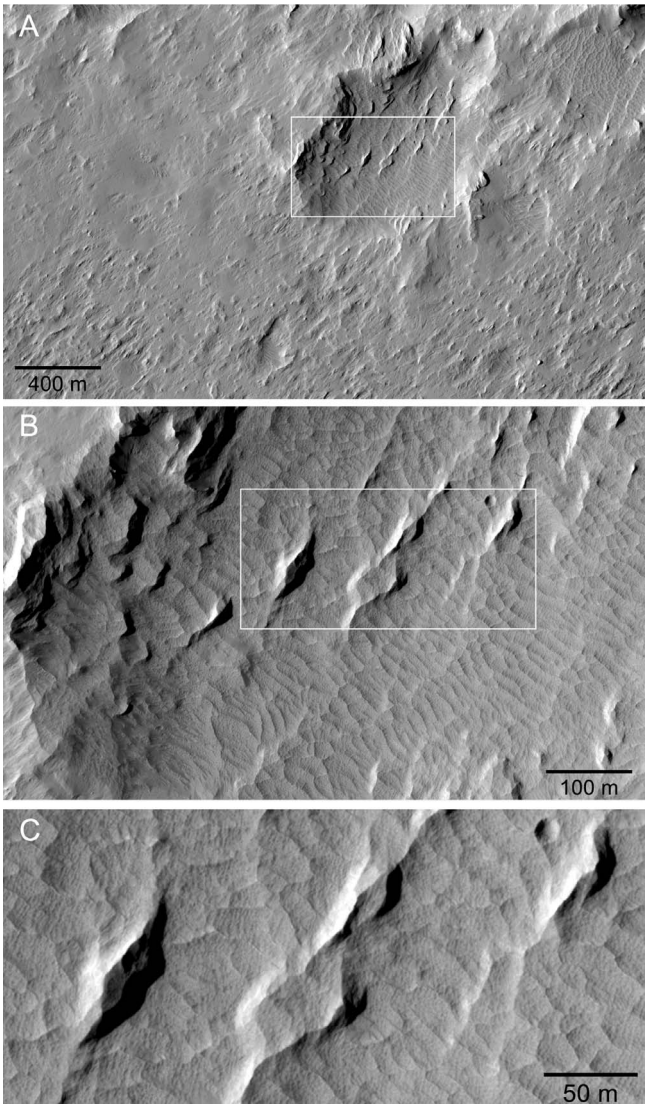

Figure 8. HiRISE image within the Medusae Fossae Formation showing periodic bedrock ridges oriented transverse to yardangs (PSP_002291_1765_RED, centered near 3.4°S, 181.5°E).

elongate tails indicate NE-SW oriented, downslope-directed winds. The floor of one of these valleys is dissected into transverse megaripple-like forms with rounded crests and asymmetric profiles (Figure 7b). Inspection of the images with the greatest enlargement (Figures 7c and 7d) reveals no suggestion of material discontinuity between the ripple forms and the neighboring streamlined fins of rock (yardangs) rising above the valley floor. This apparent lateral continuity with neighboring, eroded terrain supports the interpretation that these megaripple-like features were carved into the valley floor. Hence, that these PBRs appear to be superposed on the yardang flank in the upper center portion of the inset image (Figure 7c) implies that they were carved during active lowering of the valley bottom as the yardangs were carved. That is, the PBRs formed contemporaneously with the yardangs and thus represent a passive bed form formed during active erosion of the valley floor.

[11] PBR-like features are also carved into the Medusae Fossae Formation where megaripple-like forms occur in a local topographic depression that may be a wind-modified crater (Figure 8). Streamlining and elongation of surficial features indicates a dominant wind orientation of SW-NE across the overview image. Within the depression, a well-developed set of megaripple-like features is oriented transverse to the orientation of highstanding wind-sculpted yardangs (Figure 8b). Once again, inspection of enlargements of the image reveals no indication of any material discontinuity between the lateral transition from the megaripple-like forms and either the yardangs or the walls of the depression (Figure 8c). A crater that disrupts the megaripple pattern (Figures 8b and 8c) further indicates that the megaripple field is carved into cohesive material, although as discussed above this observation by itself does not preclude the alternative interpretation of indurated sedimentary megaripples.

[12] Another image from Ophir Chasma shows PBRs oriented transverse to streamlined yardangs carved into layered material exposed by erosion (Figure 9). Remnants of a cratered surface are apparent on the left side of the image and streamlined yardangs apparent in the lower right imply a wind direction of SE-NW. Well-defined layering in the substrate apparently runs trough to crest through a series of megaripples oriented transverse to the neighboring yardangs. Hence, these PBRs formed transverse to the dominant wind direction responsible for carving the yardangs.

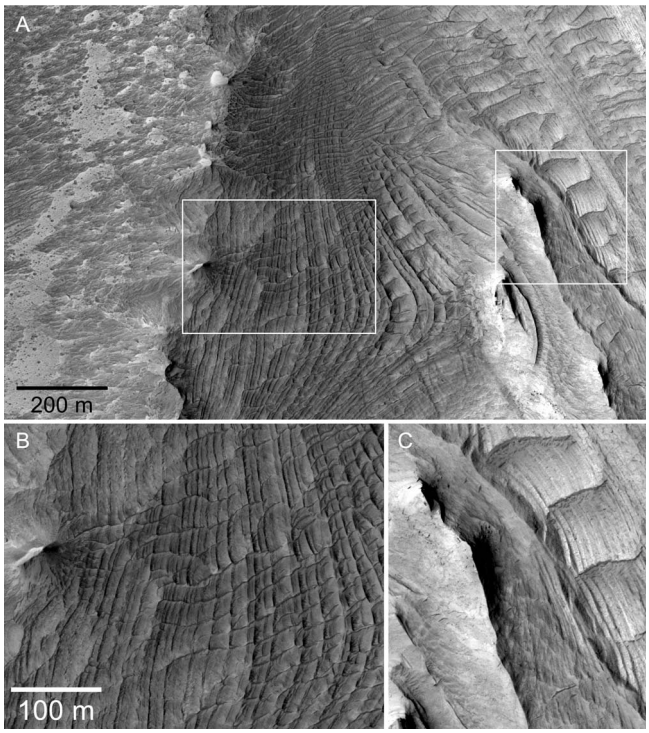

Figure 9. HiRISE image of West Ophir Chasma showing layered stratigraphy exposed from troughs to crests of periodic bedrock ridges oriented transverse to neighboring yardangs. Note remnants of cratered surface on the plains on the right side of Figure 9a. Image scales for Figures 9b and 9c are identical (ESP_015974_1760_RED, centered near 3.9°S, 285.7°E).

Table 2. Mean PBR Wavelengths (λ) Measured in Figures 2–9

Figure	Σ Length of Transects (m)	Number of PBRs	Mean λ (m)
Figure 2	1972	265	7.4 ± 0.4
Figure 3	2388	108	22.5 ± 2.7
Figure 4	5098	105	48.3 ± 9.5
Figure 5	6579	122	50.6 ± 8.0
Figure 6	5933	131	44.6 ± 8.2
Figure 7	4702	116	41.1 ± 3.5
Figure 8	3069	168	18.2 ± 1.6
Figure 9 (left)	2830	62	45.3 ± 10.1
Figure 9 (right)	1251	59	22.4 ± 7.0

Close-up images reveal bedding running continuously through numerous troughs and crests of PBRs oriented orthogonal to the wind orientation implied by the adjacent streamlined yardang (Figures 9b and 9c).

[13] The multiple lines of evidence presented above (summarized in Table 1) show that some periodic ridges within the Medusae Fossae Formation and layered deposits of Valles Marineris are eroded into bedrock by aeolian processes and form transverse to the dominant airflow. The preservation of craters disrupting sequences of megaripple-like features indicates that these features are formed in cohesive materials, and thus are not active aeolian dunes. Parallel alignment of PBRs and active sedimentary features and deflection of PBR orientation around isolated topographic features indicate that they are not exhumed and implies that they form transverse to local prevailing winds, as does the perpendicular orientation of PBRs to megayardangs in locations where both occur in proximity. A compelling observation demonstrating the erosional nature of PBRs is the presence of layered cohesive substrate exposed at the surface fully across (and thus through) sequences of megaripple-like forms. Gradational or seamless lateral transitions to yardangs and undissected surfaces further support an erosional origin for PBRs. Hence, of the previously identified dune and megaripple landforms on Mars, some are certainly not depositional features and are rather erosional landforms.

[14] The wavelengths of PBRs span a similar range as that reported for TARs [*Balme et al.*, 2008; *Berman et al.*, 2011]. We measured wavelengths of selected PBRs from the images discussed above by dividing the number of such features crossed by the length of a measured transect. Ten straight-line transects were defined on each image oriented orthogonal to PBRs and running across from 5 to 33 such features. Transects were placed both to provide relatively uniform coverage and to capture the range in PBR wavelengths expressed in each image. Each transect thus yielded a mean PBR wavelength for that transect (a local mean) that varied from 6.7 m to 66.6 m; the mean of the local means for each image ranged from 7.4 ± 0.4 m to 50.6 ± 8.0 m (Table 2). Local mean wavelength values for each transect display narrow distributions, although those from Figure 9 exhibited a bimodal distribution, reflecting the different wavelengths of PBRs apparent in Figures 9b and 9c.

3. Discussion

[15] Wind is a globally more significant agent of surface erosion on Mars than on Earth, if only because of the relative scarcity of fluvial activity. Moreover, the fluid density of the atmosphere on Mars is about 0.01 that of Earth's atmosphere, and windblown sand has far greater kinetic energy on Mars owing to higher particle velocities [*Greeley*, 2002], and thus can act as effective instruments of abrasion once set in motion [*Laity and Bridges*, 2009]. *Arvidson* [1972] proposed that the saltation flux on Mars would be greater than on Earth on the basis of scaling of the Bagnold relation (which describes the rate of sediment movement as a function of fluid densities) for Martian conditions, such as drag velocity and gravitational acceleration. Subsequent work has shown that a higher-threshold wind speed is needed to initiate aeolian transport and low wind velocities are required to sustain saltation on Mars [*Yizhaq*, 2005]. In addition, the low drag and low gravity on Mars lead to long saltation trajectories, which accelerates grains to a larger fraction of the wind velocity than on Earth; saltating grains on Mars reach velocities 5–10 times higher than those on Earth [e.g., *Almeida et al.*, 2008]. Hence, we might expect wind erosion on Mars to be a far more pervasive process than on Earth, where wind-sculpted bedrock dominates landforms in only a few, hyperarid environments. We consider the consistent transverse orientation of PBRs relative to active winds and perpendicular to yardangs in multiple images from different locations as too unlikely to be a coincidence.

[16] The common observations from the images discussed above that there are layers cropping out within the features we identified and that these layers are continuous over spatial scales larger than individual bed forms together provide strong evidence that features we term PBRs have indeed been sculpted out of bedrock. While the other, morphological arguments summarized in Table 1 are interpretive and thus do not individually invalidate interpreting these features as TARs, the multiple independent strands of consilient evidence identified above provide further support for and strengthen our conclusion that they are PBRs. Moreover, these features differ in fundamental ways from yardangs, the dominant wind-sculpted landforms on Mars.

[17] Yardangs on Earth and Mars are distinguished by a streamlined form [*McCauley*, 1973; *Ward*, 1979; *Greeley et al.*, 1992] with blunt noses facing upwind and a tapered leeward end and/or elongate sand tails [*McCauley et al.*, 1977; *El-Baz et al.*, 1979; *Greeley and Iversen*, 1985; *Ward et al.*, 1985; *Halimov and Fezer*, 1989]. Yardangs are commonly described as having the appearance of inverted ship hulls oriented in the direction of the prevailing wind [*McCauley*, 1973; *McCauley et al.*, 1977]. Although there is a range of yardang morphologies, the highest and widest part of their streamlined forms is generally about 1/3 of the way between the bow and stern in well-streamlined yardangs [*Livingstone and Warren*, 1996]. Yardangs are readily discernible from inselbergs, highstanding bedrock knobs formed through differential weathering or erosion, in that yardangs are streamlined by wind, with length-to-width ratios that range from 3:1 to 10:1 [*McCauley et al.*, 1977], whereas inselbergs are more equant. Ongoing uncertainties regarding the formation of yardangs center on their mechanisms of formation and, in particular, on the relative importance of deflation, abrasion, and weathering; but all explanations emphasize the role of an aerodynamic planform shape in controlling yardang formation and morphology.

As the PBRs described above do not exhibit such morphology, we do not consider them to potentially be yardangs.

[18] *Ward et al.* [1985] identified grooves as another wind-carved erosional form on Mars distinct from yardangs. In contrast to yardangs, grooved landforms lack streamlined form, develop on plains units, and do not exhibit bifurcation or coalescence, maintaining parallel grooves over hundreds of kilometers [*Ward*, 1979]. Ward and colleagues interpreted Martian grooves as erosionally enhanced fractures in pyroclastic units, such as an ash flow tuff. While these grooves appear to be erosional counterparts to longitudinal dunes, their orientation presumably reflects the dominant wind direction, rather than the prevalence of bidirectional winds, as sedimentary terrestrial longitudinal dunes are thought to represent [*Rubin and Hunter*, 1987].

[19] We consider PBRs to constitute another in a rich variety of aeolian erosional forms present on Mars, from megayardangs, to grooves, to the fine fish-scale texture resembling ventifact faceting that is apparent in high-resolution images of some wind-worn surfaces on Mars (for a description of the latter, see *Bridges et al.* [2010]). We interpret PBRs to be wind-carved features that, in at least several localities, lie transverse to wind directions interpreted from yardangs and active sedimentary dunes.

[20] Flow direction, orientation and substrate all influence the development of longitudinal versus transverse sedimentary dunes [see *Rubin and Hesp*, 2009; *Reffet et al.*, 2010, and references therein]. Experiments on bedform formation based on flow fields with two dominant flow orientations showed that longitudinal dunes develop when the angle between the dominant flow directions exceeds 90° and transverse dunes form when the angle between the dominant flow directions is less than 90° for both aeolian [*Rubin and Hunter*, 1987] and fluvial [*Rubin and Ikeda*, 1990] transport. Transverse bed forms (dunes and ripples) develop when subject to a single dominant, or reversing flow direction.

[21] Although it is not clear as to whether similar controls apply to the orientation of erosional landforms, it is well established in the material science literature that at much finer scales transverse ripple forms can result from abrasive erosion. Transverse erosional ripples have been documented to form on metal and ceramic surfaces due to abrasion by particles entrained in air and flowing water (Figure 10) [*Bitter*, 1963; *Finnie and Kabil*, 1965]. Particularly well studied is the formation of transverse ripples during the erosion of rubber [*Schallamach*, 1954] and metals like aluminum, copper, and lead, subject to a flux of solid particles [*Carter et al.*, 1980; *Griffin and MacMillan*, 1986; *Hovis et al.*, 1986; *Ballout et al.*, 1995; *Talia et al.*, 1996]. Similarly, studies of the effects of sandblasting on erosion of a copper surface found that for sufficiently long erosion times and impact angles of 10–65° (measured from the horizontal) a well-defined ripple pattern developed, with mass loss greatest at glancing impact angles of 10–20°

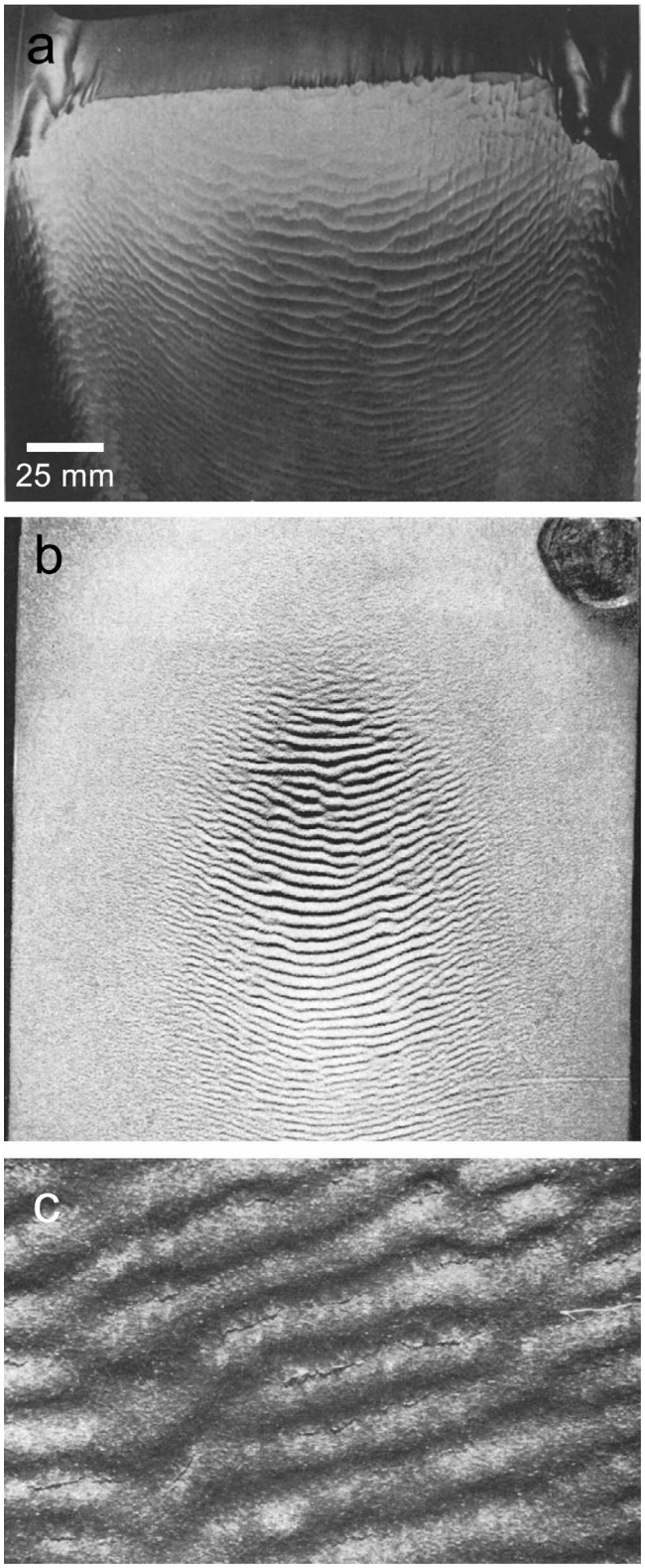

Figure 10. (a) Ripple textures eroded into an aluminum hydroelectric turbine blade; the erosion occurred owing to sediment-laden water passing over the surfaces. Adapted from *Karimi and Schmid* [1992]. (b) Aluminum eroded by sand in air; flow direction was from top to bottom. Adapted from *Finnie and Kabil* [1965]. (c) Ripples formed in silver owing to bombardment by 300 micron diameter iron particles. Adapted from *Bitter* [1963]. No scale is available for Figures 10b and 10c, although ripple-like features in both are thought to be of comparable scale to those in Figure 10a.

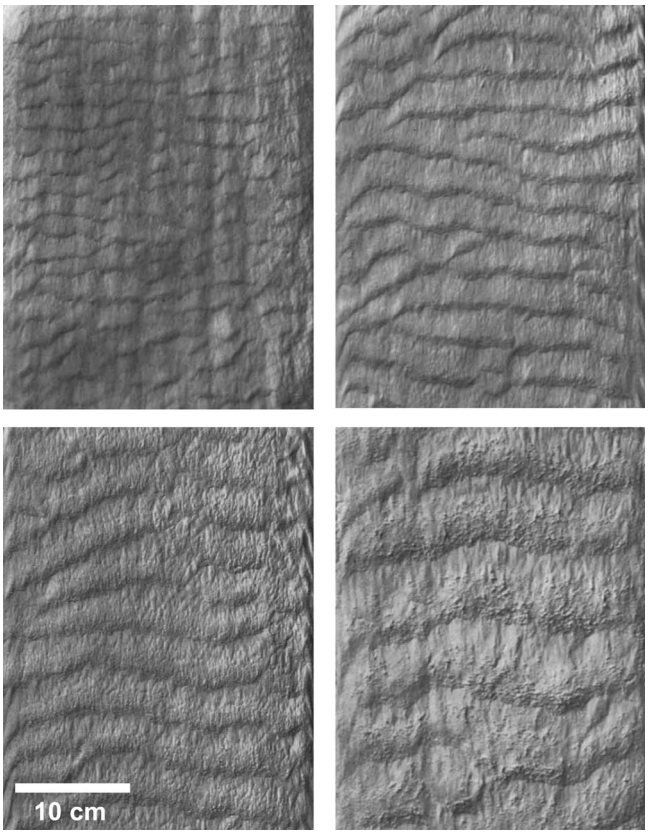

Figure 11. Plaster of Paris molds of transverse ripples formed from erosion of cohesive mud bed by high-velocity flow oriented from bottom to top from experimental runs in which a variety of wavelengths were formed using different flow velocities. Adapted from *Allen* [1971, Figures 92–95]. Conditions reported for the experimental runs shown here ranged from mean flow velocities of 33.6 to 55.2 cm s^{-1} and mean flow depths of 4.1 to 12.8 cm, with Reynolds numbers of 28,600 to 52,600 and Froude numbers of 0.30 to 0.78.

[*Carter et al.*, 1980]. The wavelength of the erosional ripple forms increased with time to an equilibrium value, upon attainment of which ripple forms were maintained as a steady-state erosional form during ongoing abrasion of the surface [*Carter et al.*, 1980]. Well-defined erosional ripples form at low impact angles and such features become smaller and less well defined at higher impact angles [*Talia et al.*, 1996]; transverse ripples form when impacts occur at angles <45°, longitudinal ripples form when impacted at angles >45°, and hill-and-valley surface topography forms when impacted at near normal angles [*Griffin and MacMillan*, 1986]. Erosional ripple formation can be prevented by continuously changing the relative wind direction [*Ballout et al.*, 1995]. These fine-scale studies demonstrate the potential for unidirectional flows of particle-laden air and water to generate a rippled morphology on an eroding surface. Could a similar, albeit far larger-scale, morphology develop from aeolian erosion of cohesive substrates on Mars?

[22] While such microabrasion provides an illustrative case, the tremendous scale difference between microabrasion and the formation of PBRs on the Martian surface means that understanding the latter will require incorporation of additional physical parameters. For example, in sand blasting the particles travel at high velocity in linear paths closely coupled to the fluid flow, whereas the path of saltating sand is much less closely coupled to the wind. Recognition of the erosional nature of PBRs is but the first step in ascertaining the appropriate physics to incorporate into models of their development.

[23] A potential terrestrial analog for PBRs is offered by aeolian megaripples with >40 m wavelengths and amplitudes >2 m reported from the Argentine Puna Plateau [*Milana*, 2009] that have been argued to be partially carved into cohesive ignimbrites [*de Silva*, 2010; *Milana et al.*, 2010]. Erosional transverse ripple-like features also have been described as resulting from abrasive fluvial erosion of cohesive substrates [*Allen*, 1969, 1971] and on bedrock streambeds [*Richardson and Carling*, 2005].

[24] *Allen* [1971] reported that erosion by high-velocity flow formed transverse erosional marks resembling sand ripples in cohesive (mud) beds owing to the spacing of flow separation along the bed interface (Figure 11). He reported that dimensional analysis of passive bed-flow interactions predict the wavelength of erosional bed forms to vary inversely with flow velocity for large channels (where the channel dimensions are far greater than the bed form wavelengths):

$$\lambda = K\mu/\rho U \tag{1}$$

where λ is the bed-feature wavelength, K is an empirical constant, μ is the dynamic viscosity of the fluid, ρ is the fluid density, and U is mean flow velocity. Observations of such features formed by water flow over limestone and airflow over ice suggest that K = 22,550 provides a reasonable terrestrial calibration [*Allen*, 1971]. Incorporating this value into equation (1) with the dynamic viscosity ($\mu = 1.115 \times 10^{-5}$ kg m^{-1} s^{-1}) and density (ρ = 0.0165 kg m^{-3}) of the Martian atmosphere (Mars datum, 220°K) predicts the wavelengths of primary erosional features expected to form by wind erosion on the Martian surface as a function of mean wind speed.

[25] Wind velocity will vary with elevation above the surface until freestream is reached. While wind velocities of >10 m s^{-1} at several m height to >45 m s^{-1} at 10 m height are required to initiate saltation on Mars [*Sullivan et al.*, 2000; *Kok*, 2010], wind speeds capable of sustaining saltation are roughly an order of magnitude less [*Kok*, 2010]. For a boundary layer problem the shear velocity (or wind friction speed, u_*) is most pertinent, and values of 1 to 3 m s^{-1} have been reported as capable of supporting aeolian sediment transport on Mars [*Sullivan et al.*, 2005; *Almeida et al.*, 2008; *Kok*, 2010]. For U = 1–3 m s^{-1} and K = 22,550 equation (1) predicts that λ = 5–15 m, values on the low end of PBR wavelengths we observed. However, further experimental and observational work is necessary to have confidence in calibrating both K and the appropriate range of effective wind velocities in this simplistic model based on dimensional analysis. Moreover, the inverse relation between bed form wavelength and wind speed predicted by equation (1) contrasts with the positive correlation of higher average wind speed with longer wavelength for

sedimentary wind ripples [e.g., *Bagnold*, 1941; *Seppälä and Lindé*, 1978]. Clearly, further work is needed to investigate the physics governing PBR development and to frame and develop more sophisticated models for understanding the processes and conditions under which PBRs form on Mars.

[26] Nonetheless, aeolian erosion into cohesive substrate offers the simplest explanation of PBRs on Mars. The lack of a streamlined form or taper is inconsistent with interpreting PBRs as yardangs and their parallel alignment with active sedimentary megaripples and orientation perpendicular to local yardangs and megayardangs shows that PBRs form transverse to the winds that carved them. In the examples discussed above, PBR crests appear orthogonal to modeled wind directions within Valles Marineris [*Spiga and Forget*, 2009]. Wind directions commonly reverse diurnally within the chasmata and many regions are dominated by anabatic and katabatic slope winds where topographic features are most prominent. Candor Chasma in particular experiences strong channelized afternoon near-surface winds and many surfaces are dominated by a single strong wind direction.

[27] The interpretation that these PBRs are carved into relatively weak materials is supported by their association in some locations with the apparent breaching of a resistant capping layer (Figures 4 and 9). A possible origin of PBRs is initial seeding by active aeolian dunes, where surface lowering preserved inherited aeolian sedimentary morphologies as incision progressed into cohesive substrate upon depletion of the surficial sediment supply. We favor the interpretation that abrasion by windblown particulate material is effective in sculpting exposures of weak indurated materials, such as the sulfate-bearing interior layered deposits exposed in the chasmata. The occurrence of material in active transport capping some PBR crests implies a connection between active transport and PBR formation. We suspect that, in general, aeolian sediment flux is a strong factor influencing erosional surface morphologies on Mars.

[28] On the basis of our limited search of the available images, conditions for the formation of PBRs appear to be optimal in the region of Valles Marineris and the Medusae Fossae Formation. In the examples discussed above, PBRs are found within sequences of relatively weak and easily eroded layered materials that have been the subject of considerable debate in regard to their origin [e.g., *Lucchitta et al.*, 1992; *Komatsu et al.*, 1993; *Montgomery and Gillespie*, 2005; *Okubo et al.*, 2008; *Adams et al.*, 2009; *Murchie et al.*, 2009]. Many of the PBR exposures we identified in Valles Marineris are from where exposures of weak substrate within the chasmata are subject to consistently oriented, high-velocity winds [*Tyler et al.*, 2002; *Spiga and Forget*, 2009] carrying an abundance of basaltic sand. As shown above, these features also occur within the Medusae Fossae Formation and thus it appears that wind erosion of PBRs could be a common process where favorable wind and substrate conditions exist. While TARs might become indurated by a variety of processes, such as evaporate cementation from cyclic wetting and drying, such alternative hypotheses for forming the features we interpret as PBRs face the challenge of explaining postdeposition creation of layering within TARs. We consider this unlikely because in that case such layers would be expected to be conformable with the surface of TARs, and thus would not be exposed on the surface and visibly cut through these megaripple-like features, as the images presented here clearly show.

4. Conclusions

[29] The presence of PBRs on Mars indicates that some megaripple forms and dune-like features are eroded into cohesive substrate. To our knowledge, periodic transverse aeolian erosional features have not been recognized previously to occur on the Martian surface. With the recognition that some megaripple-like forms may be eroded into cohesive material, further examination of such exposures may provide insight into the original depositional environment of the material now erosionally shaped into PBRs, information that would have otherwise been lost as a result of aeolian reworking if the topographic form were a primary sedimentary feature. Moreover, Martian megaripple-like features cannot be assumed to represent depositional environments on the basis of morphology alone owing to the resulting equifinality problem. Consequently, recognition of the erosional nature of PBRs raises the question of how many other such features are actually eroded into bedrock, and how extensive such features are on the surface of Mars. In any case, our observations extend the rich variety of erosional forms on Mars from wind-parallel yardangs to transverse PBRs and perhaps intermediate forms that collectively deserve further attention. Finally, while we in no way question the widespread occurrence of active aeolian sedimentary features, and the potential for the presence of extensive fossil dune fields on Mars, our results motivate the questions of how widespread are PBRs on Mars and how many of them have been misinterpreted as TARs or other features.

[30] **Acknowledgments.** We would like to thank the science and operations teams at JPL and UA for operating and targeting the HiRISE imager used for this study. JMARS software developed at ASU was used for analysis of various data sets. This work was partially supported by NASA MDAP grant NNX08AK52G. We thank Nathan Bridges and Matthew Balme for their constructive critiques of the manuscript.

References

Adams, J. B., A. R. Gillespie, M. P. A. Jackson, D. R. Montgomery, T. P. Dooley, J.-P. Combe, and B. C. Schreiber (2009), Salt tectonics and collapse of Hebes Chasma, Valles Marineris, Mars, *Geology*, *37*, 691–694, doi:10.1130/G30024A.1.

Allen, J. R. L. (1969), Erosional current marks of weakly cohesive mud beds, *J. Sediment. Petrol.*, *39*, 607–623.

Allen, J. R. L. (1971), Transverse erosional marks of mud and rock: Their physical basis and geological significance, *Sediment. Geol.*, *5*, 167–385, doi:10.1016/0037-0738(71)90001-7.

Almeida, M. P., E. J. R. Parteli, J. S. Andrade Jr., and H. J. Herrmann (2008), Giant saltation on Mars, *Proc. Natl. Acad. Sci. U. S. A.*, *105*, 6222–6226, doi:10.1073/pnas.0800202105.

Arvidson, R. E. (1972), Aeolian processes on Mars: Erosive velocities, settling velocities, and yellow clouds, *Geol. Soc. Am. Bull.*, *83*, 1503–1508, doi:10.1130/0016-7606(1972)83[1503:APOMEV]2.0.CO;2.

Bagnold, R. A. (1941), *The Physics of Blown Sand and Desert Dunes*, Methuen and Co., London.

Ballout, Y. A., J. A. Mathis, and J. E. Talia (1995), Effect of particle tangential velocity on erosion ripple formation, *Wear*, *184*, 17–21, doi:10.1016/0043-1648(94)06542-X.

Balme, M. R., D. C. Berman, M. C. Bource, and J. Zimbelman (2008), Transverse aeolian ridges (TARs) on Mars, *Geomorphology*, *101*, 703–720, doi:10.1016/j.geomorph.2008.03.011.

Berman, D. C., M. R. Balme, S. C. R. Rafkin, and J. R. Zimbelman (2011), Transverse aeolian ridges (TARs) on Mars II: Distributions, orientations, and ages, *Icarus*, *213*, 116–130, doi:10.1016/j.icarus.2011.02.014.

Bitter, J. G. A. (1963), A study of erosion phenomena: Part 1, *Wear*, *6*, 5–21, doi:10.1016/0043-1648(63)90003-6.

Bourke, M. C., M. Balme, R. A. Beyer, K. K. Williams, and J. A. Zimbelman (2006), Comparison of methods used to estimate the height of sand dunes on Mars, *Geomorphology*, *81*, 440–452, doi:10.1016/j.geomorph.2006.04.023.

Bourke, M. C., N. Lancaster, L. K. Fenton, E. J. Parteli, J. R. Zimbelman, and J. Radebough (2010), Extraterrestrial dunes: An introduction to the special issue on planetary dune systems, *Geomorphology*, *121*, 1–14, doi:10.1016/j.geomorph.2010.04.007.

Bridges, N. T., R. Greeley, A. F. C. Haldemann, K. E. Herkenhoff, M. Kraft, T. J. Parker, and A. W. Ward (1999), Ventifacts at the Pathfinder landing site, *J. Geophys. Res.*, *104*(E4), 8595–8615, doi:10.1029/98JE02550.

Bridges, N. T., P. E. Geissler, A. S. McEwen, B. J. Thomson, F. C. Chuang, K. E. Herkenhoff, L. P. Keszthelyi, and S. Martinez-Alonso (2007), Windy Mars: A dynamic planet as seen by the HiRISE camera, *Geophys. Res. Lett.*, *34*, L23205, doi:10.1029/2007GL031445.

Bridges, N. T., et al. (2010), Aeolian bedforms, yardangs, and indurated surfaces in the Tharsis Montes as seen by the HiRISE camera: Evidence for dust aggregates, *Icarus*, *205*, 165–182, doi:10.1016/j.icarus.2009.05.017.

Carr, M. H. (1981), *The Surface of Mars*, Yale Univ. Press, New Haven, Conn.

Carter, G., M. J. Nobes, and K. I. Arshak (1980), The mechanism of ripple generation on sandblasted ductile solids, *Wear*, *65*, 151–174, doi:10.1016/0043-1648(80)90019-8.

Chojnacki, M., D. M. Burr, J. E. Moersch, and T. I. Michaels (2011), Orbital observations of contemporary dune activity in Endeavor crater, Meridiani Planum, Mars, *J. Geophys. Res.*, *116*, E00F19, doi:10.1029/2010JE003675.

Cutts, J. A., and R. S. U. Smith (1973), Eolian deposits and dunes on Mars, *J. Geophys. Res.*, *78*(20), 4139–4154, doi:10.1029/JB078i020p04139.

de Silva, S. (2010), Comment on "The largest wind ripples on Earth," *Geology*, *38*, e218, doi:10.1130/G30780C.1.

Edgett, K. S., and M. C. Malin (2000), New views of Mars eolian activity, materials, and surface properties: Three vignettes from the Mars Global Surveyor Mars Orbiter Camera, *J. Geophys. Res.*, *105*(E1), 1623–1650, doi:10.1029/1999JE001152.

El-Baz, F., C. S. Breed, M. J. Grolier, and J. F. McCauley (1979), Eolian features in the western desert of Egypt and some applications to Mars, *J. Geophys. Res.*, *84*(B14), 8205–8221, doi:10.1029/JB084iB14p08205.

Finnie, I., and Y. H. Kabil (1965), On the formation of surface ripples during erosion, *Wear*, *8*, 60–69, doi:10.1016/0043-1648(65)90251-6.

Greeley, R. (2002), Saltation impact as a means for raising dust on Mars, *Planet. Space Sci.*, *50*, 151–155, doi:10.1016/S0032-0633(01)00127-1.

Greeley, R., and J. D. Iversen (1985), *Wind as a Geological Process on Earth, Mars, Venus, and Titan*, Cambridge Univ. Press, Cambridge, Mass., doi:10.1017/CBO9780511573071.

Greeley, R., N. Lancaster, S. Lee, and P. Thomas (1992), Martian aeolian processes, sediments, and features, in *Mars*, edited by H. H. Kieffer et al., pp. 730–766, Univ. of Ariz. Press, Tucson.

Griffin, M. J., and N. H. MacMillan (1986), Longitudinal and transverse ripple formation during the solid particle erosion of lead, *Mater. Sci. Eng.*, *80*, L1–L4, doi:10.1016/0025-5416(86)90307-1.

Halimov, M., and F. Fezer (1989), Eight yardang types in central Asia, *Z. Geomorphol.*, *33*, 205–217.

Hansen, C. J., et al. (2011), Seasonal erosion and restoration of Mars' northern polar dunes, *Science*, *331*, 575–578, doi:10.1126/science.1197636.

Hovis, S. K., J. Talia, and R. O. Scattergood (1986), Erosion mechanisms in aluminum and Al-Si alloys, *Wear*, *107*, 175–181, doi:10.1016/0043-1648(86)90026-8.

Karimi, A., and R. K. Schmid (1992), Ripple formation in solid-liquid erosion, *Wear*, *156*, 33–47, doi:10.1016/0043-1648(92)90142-U.

Kok, J. F. (2010), Difference in the wind speeds required for initiation versus continuation of sand transport on Mars: Implications for dunes and dust storms, *Phys. Rev. Lett.*, *104*, 074502, doi:10.1103/PhysRevLett.104.074502.

Komatsu, G., P. E. Geissler, R. G. Strom, and R. B. Singer (1993), Stratigraphy and erosional landforms of layered deposits in Valles Marineris, Mars, *J. Geophys. Res.*, *98*, 11,105–11,121, doi:10.1029/93JE00537.

Laity, J. E., and N. T. Bridges (2009), Ventifacts on Earth and Mars: Analytical, field, and laboratory studies supporting sand abrasion and windward feature development, *Geomorphology*, *105*, 202–217, doi:10.1016/j.geomorph.2008.09.014.

Livingstone, I., and A. Warren (1996), *Aeolian Geomorphology: An Introduction*, Pearson Longman, White Plains, N. Y.

Lucchitta, B. K., A. S. McEwen, G. D. Clow, P. E. Geissler, R. B. Singer, R. A. Schultz, and S. W. Squyres (1992), The canyon system on Mars, in *Mars*, edited by H. H. Kieffer et al., pp. 453–492, Univ. of Ariz. Press, Tucson.

Malin, M. C., and K. S. Edgett (2001), Global Surveyor Mars Orbiter Camera: Interplanetary cruise through primary mission, *J. Geophys. Res.*, *106*, 23,429–23,570, doi:10.1029/2000JE001455.

McCauley, J. F. (1973), Mariner 9 evidence for wind erosion in the equatorial and mid-latitude regions of Mars, *J. Geophys. Res.*, *78*(20), 4123–4137, doi:10.1029/JB078i020p04123.

McCauley, J. F., M. H. Carr, J. A. Cutts, W. K. Hartmann, H. Masursky, D. J. Milton, R. P. Sharp, and D. E. Wilhelms (1972), Preliminary Mariner 9 report on the geology of Mars, *Icarus*, *17*, 289–327, doi:10.1016/0019-1035(72)90003-6.

McCauley, J. F., M. J. Grolier, and C. S. Breed (1977), Yardangs, in *Geomorphology in Arid Regions*, edited by D. O. Doehring, pp. 233–269, Unwin Hyman, Crows Nest, N. S. W., Australia.

McEwen, A. S., et al. (2007), Reconnaissance Orbiter's High Resolution Imaging Science Experiment (HiRISE), *J. Geophys. Res.*, *112*, E05S02, doi:10.1029/2005JE002605.

Milana, J. P. (2009), Largest wind ripples on Earth?, *Geology*, *37*, 343–346, doi:10.1130/G25382A.1.

Milana, J. P., S. Forman, and D. Kröhling (2010), Reply to comment by J. P. Milana on "Largest wind ripples on Earth," *Geology*, *38*, e219–e220, doi:10.1130/G31354Y.1.

Montgomery, D. R., and A. Gillespie (2005), Formation of Martian outflow channels by catastrophic dewatering of evaporite deposits, *Geology*, *33*, 625–628, doi:10.1130/G21270.1.

Murchie, S., et al. (2009), Evidence for the origin of layered deposits in Candor Chasma, Mars, from mineral composition and hydrologic modeling, *J. Geophys. Res.*, *114*, E00D05, doi:10.1029/2009JE003343.

Okubo, C. H., K. W. Lewis, A. S. McEwen, and R. L. Kirk (2008), Relative age of interior layered deposits in southwest Candor Chasma based on high-resolution structural mapping, *J. Geophys. Res.*, *113*, E12002, doi:10.1029/2008JE003181.

Reffet, E., S. Courrech du Pont, P. Hersen, and S. Douady (2010), Formation and stability of transverse and longitudinal sand dunes, *Geology*, *38*, 491–494, doi:10.1130/G30894.1.

Richardson, K., and P. A. Carling (2005), A typology of sculpted forms in open bedrock channels, *Spec. Pap. Geol. Soc. Am.*, *392*, 1–108.

Rubin, D. M., and P. A. Hesp (2009), Multiple origins of linear dunes on Earth and Titan, *Nat. Geosci.*, *2*, 653–658, doi:10.1038/ngeo610.

Rubin, D. M., and R. E. Hunter (1987), Bedform alignment in directionally varying flows, *Science*, *237*, 276–278, doi:10.1126/science.237.4812.276.

Rubin, D. M., and H. Ikeda (1990), Flume experiments on the alignment of transverse, oblique, and longitudinal dunes in directionally varying flows, *Sedimentology*, *37*, 673–684, doi:10.1111/j.1365-3091.1990.tb00628.x.

Schallamach, A. (1954), On the abrasion of rubber, *Proc. Phys. Soc. London, Sect. B*, *67*, 883–891, doi:10.1088/0370-1301/67/12/304.

Seppälä, M., and K. Lindé (1978), Wind tunnel studies of ripple formation, *Geogr. Ann., Ser. A*, *60*, 29–42, doi:10.2307/520963.

Silvestro, S., L. K. Fenton, D. A. Vaz, N. T. Bridges, and G. G. Ori (2010), Ripple migration and dune activity on Mars: Evidence for dynamic wind processes, *Geophys. Res. Lett.*, *37*, L20203, doi:10.1029/2010GL044743.

Spiga, A., and F. Forget (2009), A new model to simulate the Martian mesoscale and microscale atmospheric circulation: Validation and first results, *J. Geophys. Res.*, *114*, E02009, doi:10.1029/2008JE003242.

Sullivan, R., R. Greeley, M. Kraft, G. Wilson, M. Golombek, K. Herkenhoff, J. Murphy, and P. Smith (2000), Results of the Imager for Mars Pathfinder windsock experiment, *J. Geophys. Res.*, *105*, 24,547–24,562, doi:10.1029/1999JE001234.

Sullivan, R., et al. (2005), Aeolian processes at the Mars Exploration Rover Meridiani Planum landing site, *Nature*, *436*, 58–61, doi:10.1038/nature03641.

Talia, J. E., Y. A. Ballout, and R. O. Scattergood (1996), Erosion ripple formation mechanism in aluminum and aluminum alloys, *Wear*, *196*, 285–294, doi:10.1016/0043-1648(96)06928-1.

Thomson, B. J., N. T. Bridges, and R. Greeley (2008), Rock abrasion features in the Columbia Hills, Mars, *J. Geophys. Res.*, *113*, E08010, doi:10.1029/2007JE003018.

Tyler, D., Jr., J. R. Barnes, and R. M. Haberle (2002), Simulation of surface meteorology at the Pathfinder and VL1 sites using a Mars mesoscale model, *J. Geophys. Res.*, *107*(E4), 5018, doi:10.1029/2001JE001618.

Ward, A. W. (1979), Yardangs on Mars: Evidence of recent wind erosion, *J. Geophys. Res.*, *84*, 8147–8166, doi:10.1029/JB084iB14p08147.

Ward, A. W., K. B. Doyle, P. J. Helm, M. K. Weisman, and N. E. Witbeck (1985), Global map of eolian features on Mars, *J. Geophys. Res.*, *90*, 2038–2056, doi:10.1029/JB090iB02p02038.

Wilson, S. A., and J. R. Zimbelman (2004), Latitude-dependent nature and physical characteristics of transverse aeolian ridges on Mars, *J. Geophys. Res.*, *109*, E10003, doi:10.1029/2004JE002247.

Yizhaq, H. (2005), A mathematical model for aeolian megaripples on Mars, *Physica A*, *357*, 57–63, doi:10.1016/j.physa.2005.05.070.

Zimbelman, J. R. (2000), Non-active dunes in the Acheron Fossae region of Mars between the Viking and Mars Global Surveyor eras, *Geophys. Res. Lett.*, *27*(7), 1069–1072, doi:10.1029/1999GL008399.

Zimbelman, J. R. (2010), Transverse aeolian ridges on Mars: First results from HiRISE images, *Geomorphology*, *121*, 22–29, doi:10.1016/j.geomorph.2009.05.012.

J. L. Bandfield, S. K. Becker, and D. R. Montgomery, Department of Earth and Space Sciences, University of Washington, 4000 15th Ave. NE, Seattle, WA 98195-1310, USA. (dave@ess.washington.edu)